PHYSICAL REVIEW E **103**, 013208 (2021)

Statistical physics of two-temperature rotational energy distributions in stationary plasmas

Marco Antonio Ridenti,[*] Jayr de Amorim, and Carlos Alberto Bomfim Silva
Department of Physics, ITA-Aeronautics Institute of Technology, São José dos Campos 12228-900, Brazil

Jan Voráč
Department of Physical Electronics, Faculty of Science, Masaryk University, Kotlářská 2, 611 37 Brno, Czech Republic

Carlos Eduardo Fellows and Laiz Rodrigues Ventura
Departamento de Física, Instituto de Ciências Exatas-ICEx, Universidade Federal Fluminense, Campus do Aterrado,
Volta Redonda, Rio de Janeiro 27213-145, Brazil

(Received 6 October 2020; accepted 22 December 2020; published 14 January 2021; corrected 2 February 2021)

Two-temperature rotational energy distributions from rarefied diatomic molecules are very often observed in laboratory plasmas. There has been much debate over the years about the physical meaning of this kind of rotational energy distributions and the associated statistical physics. We show here that under certain reasonable assumptions and constraints the condition of Shannon-Jaynes entropy maximization may produce a two-temperature distribution. This may happen, for instance, when a system is simultaneously coupled to different thermal baths. In plasmas this is possible because rarefied molecular species may be immersed in a medium where electrons and the dominant atomic species are quasidecoupled, each of them acting as distinct thermal baths. Considering that molecular species may interact both with electrons and heavy neutral species, we may ask what should be the resulting molecular energy distribution. We answer this question in this paper and give some examples on how this can be used to interpret experimental molecular distribution from partially ionized plasmas.

DOI: 10.1103/PhysRevE.103.013208

I. INTRODUCTION

The use of rovibrational emission spectra from plasma sources is a very old and well-established technique to estimate the temperature of an emitting media in thermodynamic equilibrium [1]. Indeed, the validity of this technique requires, at least, that rotational states are in thermodynamic equilibrium with the dominant species [1]. However, this condition may not be fulfilled since many systems of interest in plasma physics deviate from equilibrium to some degree [2,3]. For this reason, the analysis of the validity of this technique requires sufficient knowledge of the equilibrium state of the plasma, which could be inferred from complementary experimental evidence [4]. For instance, this could be achieved from the analysis of other spectra, such as electronic emission. If both electronic and rovibrational spectra exhibit an equilibrium distribution with the same temperature, then probably the media is in thermodynamic equilibrium.

In some cases where the deviation from equilibrium is observed, the neutral, ion, and electron velocity distributions may be well approximated by Maxwellians having distinct temperatures. Depending on the degree of deviation, also neutral species may have distinct velocity, electronic, vibrational, and rotational distributions. In such nonequilibrium states it may not be possible to identify a well defined temperature. The parameter temperature may still be used is this new context, but it must be given a new definition.

In partially ionized plasmas, commonly used in technological applications, ions, and electrons velocity distributions always have different mean kinetic energies [3,5]. In the case of low power density and partially ionized plasmas, electrons gain energy from the electric field and lose energy in collisions with neutral heavy species [6]. The gas of heavier particles (mass M) will never reach thermodynamic equilibrium with electrons (mass m) because the electron transfers only a tiny amount of kinetic energy to its heavier collisional partner ($\sim m/M$) [7,8], and the density of electrons is much smaller than the density of neutral species (partially ionized plasma). Although heavier particles absorb energy, the electrons' heating rate is not high enough to overcome the cooling rate, and the resulting steady-state electron velocity distribution deviates from the gas velocity distribution, having a higher mean energy [6]. The system reaches the steady condition through improper balances [9]. Only in the case where the electron field is a tiny perturbation, i.e., the electric field power transfer is much smaller than the energy exchange rate by collisions, then the system may reach equilibrium. Only in this condition the linear response theory applies [10].

In systems we are describing and which are commonly found in plasma applications, electrons, and neutral heavy species, have different mean energies. What could we say about ions? Ions transfer a significant part of their energy to their collisional partners and typically have a mean free path much smaller than the one from electrons. Ions will indeed

---

[*] aridenti@ita.br

gain some energy from the field but at a lower rate [6]. They also lose energy at a higher loss rate through collisions [6]. For that reason, the ion mean energy is expected to be only slightly higher than the neutral species mean energy.

The velocity distribution of electrons and heavy species does not need to be Maxwellian [10,11]. However, experimental evidence usually confirms that very often they can be approximated by equilibrium distributions with well defined temperatures [12]. In the case of heavy species this is well justified by the fact that the input energy rate from electrons is much smaller than the energy exchange rate in collisions between heavy species. In the case of electrons, it is expected that a depletion of the tail of the kinetic energy distribution function occurs near the ionization and excitation (electronic or vibrational) threshold [3,6,11]. Below the minimum threshold for inelastic collisions, the distribution is then expected to resemble a Maxwellian with an effective temperature much higher than the temperature of heavy species [12–15]. Above the minimum threshold, the distribution tends to be depleted [15,16]. If the electron density is sufficiently high, collisions between electrons contribute to populate the depleted tail, producing a Maxwellian distribution with a lower temperature [16,17] but still higher than the temperature of heavy species.

The plasmas we have been describing so far have a remarkable feature: Neutral species and electrons have quite different mean energies so that we may call them "two-temperature" plasmas. Indeed, a two-temperature plasma may be seen as a composition of two thermal baths. Although there is some coupling between electrons and neutrals, we may neglect it and consider both systems as being independent. Any other minor constituent of the plasma, such as excited molecules or atoms, radicals, and ions could be coupled to both thermal baths. In this paper we are interested in rotational states of diatomic molecules, and we could formulate our central question in the following way: What should be the steady-state rotational energy distribution of a diatomic molecule present in a two-temperature plasma at very low relative concentration if it may couple to both thermal baths?

The physical conditions which we have just described are common and have been observed before. Many experimental works discuss the nonequilibrium rovibrational distributions which occur in low power density partially ionized plasmas. These are mainly the rotational distributions of OH(A), $N_2^+(B)$, and $N_2(C)$, which give rise to the well known OH violet system, N_2^+ first negative system, and N_2 second positive system [1,18].

Some authors argue that such systems result from the composition of two subsystems, each of them coupled to the corresponding thermal bath [19,20]. The molecular rotational energy distribution function of diatomic molecules would be the result of the linear combination of two equilibrium distributions, i.e.,

$$N(E_i) = I_1 \frac{e^{-E_i/k_B T_1}}{Z_1} + I_2 \frac{e^{-E_i/k_B T_2}}{Z_2}, \tag{1}$$

where $N(E_i)$ is the population of states with energy E_i; Z_1, Z_2, T_1, and T_2 are the partition functions and temperatures of the thermal baths 1 and 2, I_1 and I_2 are weighting factors, and k_B is the Boltzmann constant. Although this result seems plausible, the reasoning behind this result should be subject to greater scrutiny.

Firstly, we should ask if Eq. (1) could be derived from first principles, i.e., the maximization of Boltzmann-Gibbs entropy or the larger and powerful scheme of Jaynes predictive statistical mechanics [21] based on the Bayesian method in probability theory together with the principle of maximization of Shannon-Jaynes entropy [22,23]. As far as we know, such a distribution has always been proposed in an *ad hoc* fashion. This approach would be perfectly valid in an experiment where two separated plasma volumes emit rovibrational spectra from the same emission system. But in this case the plasma would not be an authentic two-temperature system; it is just two separate systems in different thermal baths emitting light simultaneously. The situation discussed here is quite different: One plasma constituent interacts with two distinct thermal baths.

The potential problems in Eq. (1) can be seen at first glance if we consider the high and low energy limits. It is reasonable to assume that at low energies the rotational states should be coupled to the main neutral species via collisions [24]. The rotational relaxation rate due to collisions with the dominant species is known to decrease exponentially with the rotational number [24]. The rotational energy distribution is then expected to approach equilibrium, i.e., $N(E_i) \sim I_1 e^{-E_i/k_B T_1}/Z_1$, where $E_i \ll k_B T_2$. However, in this limit Eq. (1) tends to $N(E_i) \sim I_1 e^{-E_i/k_B T_1}/Z_1 + I_2$. If I_2 is not too much smaller than I_1, then the estimate of T_1 based on Eq. (1) could yield severely biased values. For this reason, some authors prefer to fit a Boltzmann distribution in the low energy limit and another Boltzmann distribution in the high energy limit [25]. This procedure is correct in our opinion, and it is consistent with our results as we will show later.

Some authors used the so-called nonextensive statistics of Tsallis to tackle the same problem [26]. Here, the entropy S_q of Tsallis is supposed to give the correct description of the system or, at least, a legitimate alternative description. The distribution resulting from this method depends not only on the temperature, but also on the so-called nonadditivity parameter q. This distribution can be used to fit experimental data as well as Eq. (1). However, the physical meaning of q in this context is still obscure since it is not clear why one should resort to a nonadditive entropy. Also, the theory does not answer how parameter q is related to the microdynamics. The temperature T, for instance, has a very clear physical interpretation as a quantity proportional to the mean kinetic energy. But what is q and what could it tell us about the physical system?

Maybe there is a rigorous justification for the application of Tsallis statistics in this context, which could certainly add an insightful contribution to the understanding of the system. However, the well-established statistical methods based on informational Shannon-Jaynes entropy and Jaynes principle are always valid as long as all the relevant constrained variables can be identified. One may question if the composition law—implicit on the derivation of informational Shannon-Jaynes entropy—should always be valid. We do not have any evidence that this should break apart in our system, nor the proponents of Tsallis statistics have shown why it should break apart. Anyway, there is always some way of defining a complete set of microstates in such a way they are all independent. For instance, one particle or few particle states may indeed be correlated to other particle states. However, the full particle states are always uncorrelated if the system is memoryless, which is the case for almost all problems in physics. We will not need to go too far as we will see that the present system can indeed be described on the basis of orthodox statistical physics considering one particle microstates. By this argument we are in no way demeaning or criticizing Tsallis statistics; as any other method in physics, the conditions where its application is valid, legitimate, and useful should always be discussed.

Before proceeding, we should note that we are neglecting an effect which could certainly affect the rotational energy distribution: the formation process. The diatomic molecule is usually formed in the plasma via chemical reactions or electronic interactions, some of which may be exothermic. Just after formation, the exceeding energy may be distributed among the rotational energy levels in a particular way, depending on the nature and statistics of the formation process. Another similar effect is the vibrotational transfer, which excites high energy rotational states and populates the tail of the rotational distribution. These effects could be strong enough to compete with rotational energy redistribution via collisional rotational transfer relaxation. We treated these cases in a previous paper where we derived the rotational energy distribution of molecules that were coupled to a thermal bath but also subject to the energy output from formation processes [27]. Now, in this paper, we neglect these effects. This is valid as long as the molecular excited states created after the formation processes are rapidly damped by collisions or the formation process is not determined by an exoergic reaction. Instead, the excitation/deexcitation of the rotational states is determined by the interaction with a thermal bath, such as the interaction with a given population of electrons or neutral species in thermal equilibrium.

In this paper we study the rotational distribution of a diatomic molecule in contact with two thermal baths by maximizing the associated Shannon-Jaynes entropy under some constraints, which will be made explicit in the next section. In our opinion, this is the most straightforward way to solve the problem. In order to validate our method, we propose an alternative derivation, based on the master equations, following the method proposed in our previous work [27].

II. THEORY

A. Derivation from Shannon-Jaynes entropy maximization

Let us consider a system $\mathfrak{S}$ which is coupled to two decoupled thermal baths $\mathfrak{T}_1$ and $\mathfrak{T}_2$ as represented in Fig. 1. The thermal baths are assumed to have constant temperatures T_1 and T_2 and an arbitrarily high heat capacity so that energy exchange with $\mathfrak{S}$ does not change T_1 and T_2. Besides, thermal baths $\mathfrak{T}_1$ and $\mathfrak{T}_2$ are decoupled from each other, i.e., they only exchange energy with system $\mathfrak{S}$ but not among themselves. Assuming that such a system is in equilibrium, we will derive the energy distribution of the microscopic discrete states of the system.

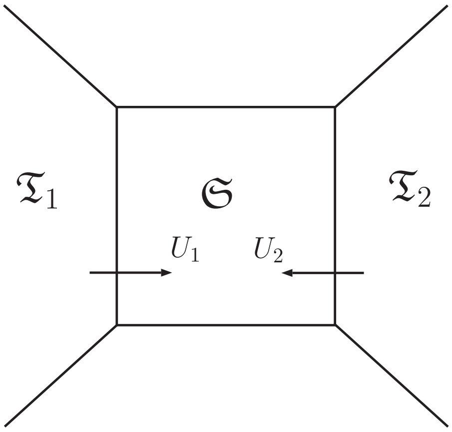

FIG. 1. System $\mathfrak{S}$ is coupled to thermal baths $\mathfrak{T}_1$ and $\mathfrak{T}_2$. The total mean energy of system $\mathfrak{S}$ is $U = U_1 + U_2$, where U_1 and U_2 are the partial contributions from thermal baths $\mathfrak{T}_1$ and $\mathfrak{T}_2$ to the total internal energy U.

The total mean energy of system $\mathfrak{S}$ is $U = U_1 + U_2$, where U_1 and U_2 are the partial contributions from thermal baths $\mathfrak{T}_1$ and $\mathfrak{T}_2$ to the total internal energy U. This means that the energy which populates the microscopic discrete states of the system by means of heat exchange either comes from thermal bath $\mathfrak{T}_1$ or comes from thermal bath $\mathfrak{T}_2$. The partial energies U_1 and U_2 are equilibrium quantities that depend only on the temperatures of the thermal baths and the energy flow from the bath to the system $\dot{Q}_i(t) = T_i\dot{S}_i(t)$. Given two thermal baths with temperatures T_1 and T_2, the equilibrium values U_1 and U_2 do not depend on the path from some initial value U_{01} or U_{02} ($U_0 = U_{01} + U_{02}$). These statements are proven in Appendix A from some general assumptions that should be valid for the present case. Since the thermal baths have well defined temperatures T_1 and T_2, we may define them in terms of the system total entropy S as

$$\left(\frac{\partial S}{\partial U_1}\right)_{U_2} = \frac{1}{T_1}, \tag{2a}$$

$$\left(\frac{\partial S}{\partial U_2}\right)_{U_1} = \frac{1}{T_2}. \tag{2b}$$

Here we are implicitly assuming that microstates of the system are discrete. Any energy level j has a probability of occupation p_j, and the sum over all states should be equal to one, i.e.,

$$\sum p_j = 1. \tag{3}$$

The total mean internal energy is given by the summation of the energy E_j times the occupation probability p_j,

$$U = \sum p_j E_j. \tag{4}$$

Equations (3) and (4) are standard and straightforward, but now we will give a step forward to add some new constraints required by our problem.

For any occupied state j, we could define the probability $K_j^{(1)}$, which is the probability of the state being populated by the interaction with thermal bath $\mathfrak{T}_1$. Analogously, we define the probability $K_j^{(2)}$, which is the probability of the state being populated by the interaction with thermal bath $\mathfrak{T}_2$. From these definitions we may write the mean energies U_1 and U_2 as

$$U_1 = \sum_j K_j^{(1)} p_j E_j, \tag{5a}$$

$$U_2 = \sum_j K_j^{(2)} p_j E_j, \tag{5b}$$

where $K_j^{(1)} + K_j^{(2)} = 1$ for all j. We may now maximize the Shannon-Jaynes entropy $S = -k_B \sum p_j \ln p_j$ subject to the constraints given by Eqs. (3), (5a), and (5b). We recall here that U_1 and U_2 are well defined and measurable quantities, so the constraints (5a) and (5b) are valid. The functional to be maximized may be written as

$$\begin{aligned} S(\{p_j\}, \lambda_0, \lambda_1, \lambda_3) = -k_B \sum p_j \ln p_j - \lambda_0 \left(\sum_j p_j - 1 \right) \\ - \lambda_1 \left(\sum_j \left(1 - K_j^{(2)}\right) p_j E_j - U_1 \right) \\ - \lambda_2 \left(\sum_j K_j^{(2)} p_j E_j - U_2 \right), \end{aligned} \tag{6}$$

where λ_0, λ_1, and λ_3 are the Lagrangian multipliers associated with the constraints given by Eqs. (3), (5a), and (5b). By applying the variational principle we find

$$p_j = \exp\left(-1 - \frac{\lambda_0}{k_B} - \frac{\lambda_1}{k_B}\left(1 - K_j^{(2)}\right) E_j - \frac{\lambda_2}{k_B} K_j^{(2)} E_j \right). \tag{7}$$

The normalization condition expressed by Eq. (3) may be used to eliminate the multiplier λ_0 and rewrite Eq. (7) as

$$p_j = \frac{1}{Z} \exp\left(- \sum_{k=1,2} \lambda_k g_{kj} \right), \tag{8}$$

where $g_{kj} = K_j^{(k)} E_j / k_B$ and

$$Z = \sum_j \exp\left(- \sum_{k=1,2} \lambda_k g_{kj} \right). \tag{9}$$

We may now write the entropy using the expression for p_j given by Eq. (8),

$$\begin{aligned} S &= k_B \ln Z + \lambda_1 \sum_j \frac{1}{Z}\left(1 - K_j^{(2)} E_j\right) \exp\left(- \sum \lambda_k g_{kj} \right) \\ &\quad + \lambda_2 \sum_j \frac{1}{Z} K_j^{(2)} E_j \exp\left(- \sum \lambda_k g_{kj} \right) \\ &= k_B \ln Z + \lambda_1 U_1 + \lambda_2 U_2. \end{aligned} \tag{10}$$

From the relations between entropy and temperature expressed by Eqs. (2a) and (2b) we may determine the remaining Lagrangian multipliers λ_1 and λ_2

$$\lambda_1 = \frac{1}{T_1}, \tag{11a}$$

$$\lambda_2 = \frac{1}{T_2}. \tag{11b}$$

The Lagrangian multipliers λ_1 and λ_2 are nothing but the inverse of the thermal baths temperatures T_1 and T_2. Now we can write the final expression for the probability distribution function,

$$p_j = \frac{\exp\left(-\left(1 - K_j^{(2)}\right) \frac{E_j}{k_B T_1}\right) \exp\left(-K_j^{(2)} \frac{E_j}{k_B T_2}\right)}{\sum_i \exp\left(-\left(1 - K_i^{(2)}\right) \frac{E_i}{k_B T_1}\right) \exp\left(-K_i^{(2)} \frac{E_i}{k_B T_2}\right)}. \tag{12}$$

The distribution function of the system is actually the product of two-exponential functions having different temperatures T_1 and T_2 and not the sum of two-exponential functions. The values of $K_j^{(1,2)}$ are not necessarily independent of state j, and some states can be better coupled to one thermal bath than the other. For simplicity, let us take a particular case and assume that for a given $j = j_{\text{th}}$ we have

$$\begin{aligned} K_j^{(1)} &= 1 \quad \text{and} \quad K_j^{(2)} = 0 \quad \text{for } j < j_{\text{th}}, \\ K_j^{(1)} &= 0 \quad \text{and} \quad K_j^{(2)} = 1 \quad \text{for } j \geqslant j_{\text{th}}. \end{aligned} \tag{13}$$

This simplified model tells that states for which $j < j_{\text{th}}$ couple only to thermal bath $\mathfrak{T}_1$ and states for which $j \geqslant j_{\text{th}}$ couple only to thermal bath $\mathfrak{T}_2$. In this particular case, the probability distribution function reduces to a Boltzmann one with temperature T_1 for states satisfying $j < j_{\text{th}}$ and another Boltzmann distribution with temperature T_2 for states satisfying $j \geqslant j_{\text{th}}$. This model is consistent with the distribution of rotational states of rarefied molecules in plasmas where rotational states are better coupled to translational motion at low lying energy levels and better coupled to electrons at upper lying energy levels.

If the values of $K_j^{(1,2)}$ are equiprobable (i.e., $K_j^{(1)} = K_j^{(2)} = 0, 5$) and independent of the states, then the distribution function also reduces to a Boltzmann one with an effective temperature equal to the harmonic mean of T_1 and T_2. Such a limit does not have any similarity with the problem we are studying but may find other applications in physics.

We may need to consider a continuous transition between thermal baths $\mathfrak{T}_1$ and $\mathfrak{T}_2$ when working with experimental spectra. In this paper, we use the following function to model $K_j^{(1)}$ and $K_j^{(2)}$:

$$\begin{aligned} K_j^{(1)} &= \frac{1}{2} \text{erfc}\left[\left(\frac{\tilde{E}_0 - E_j}{\tilde{\sigma}_0 \sqrt{2}} \right) \right], \\ K_j^{(2)} &= \frac{1}{2} \text{erfc}\left[\left(\frac{E_j - \tilde{E}_0}{\tilde{\sigma}_0 \sqrt{2}} \right) \right], \end{aligned} \tag{14}$$

where $\tilde{E}_0$ and $\tilde{\sigma}_0$ are parameters to be determined and erfc is the complementary error function. The $\tilde{E}_0$ value gives a measure of the transition energy between thermal baths, whereas $\tilde{\sigma}_0$ determines how steep is the transition. The choice of the $K_j^{(i)}$ expressions is not unique, but this particular form [Eq. (14)] satisfies some plausible assumptions about the system we want to investigate. The first requirement is that in the low and high energy limits we have $K_j^{(1)} = 1$, $K_j^{(2)} = 0$ and $K_j^{(1)} = 0$, $K_j^{(2)} = 1$, respectively. The second requirement imposes that the transition between both extreme cases could be smooth and not necessarily steep as in the case of Eq. (13). Because of our prior ignorance we should assume that the transition is symmetric, which is the third requirement. Lastly, since the function erfc(x) may be directly linked to the probability that a given state couples to a given thermal bath, the sums $K_j^{(1)}$ and $K_j^{(2)}$ should always be equal to unity for every j. The erfc(x) function allows us to control the steepness of the transition by changing the value of parameter $\tilde{\sigma}_0$, and it assures that the third and fourth requirements are met. Many other cumulative distribution functions (CDFs) could possibly be chosen, however, due to our prior ignorance, the erfc(x) function is a good choice since it is the CDF of a normal distribution, the most natural choice for a probability distribution function due to the central limit theorem.

B. Derivation using the rate equations

In this section we will derive essentially the same result but using a different approach, which we have adopted earlier in another paper [27]. This derivation is based on the rate equations describing the excitation of molecular rotational states from collisions with atoms and electrons, which we will call rotational energy transfer (RET). As we have already shown in our previous paper [27], the process of the RET in an OH(A, $\nu = 0$)[1] containing plasma or gas whose dominant species is an arbitrary atom or molecule MN may be represented by the equations

$$M_j + \mathrm{OH}(A)_{i+1} \underset{k'^{i,(+)}_{M,j+1}}{\overset{k^{i+1,(+)}_{M,j}}{\rightleftharpoons}} M_{j+1,(+)} + \mathrm{OH}(A)_i, \qquad (15)$$

$$M_j + \mathrm{OH}(A)_{i} \underset{k'^{i-1,(-)}_{M,j+1}}{\overset{k^{i,(-)}_{M,j}}{\rightleftharpoons}} M_{j+1,(-)} + \mathrm{OH}(A)_{i-1}, \qquad (16)$$

where the subscript j (or $j+1$) means that species M has a kinetic energy E_j (or $E_j + \Delta E^{(+,-)}$) and the subscript i represents the rotational level OH($A, J = i$). The (+) superscript refers to a transition of the kind $i+1 \rightleftharpoons i$ and the (−) superscript refers to a transition of the kind $i \rightleftharpoons i-1$. This exhausts all the possibilities of population and depopulation of a given rotational state i by a RET process. In the case we treat in this paper, the species M is the dominant constituent of the background gas, which is an atom for simplicity.

We consider now the RET caused by the interaction of the diatomic molecules with electrons, which we will call the electronic RET. The corresponding rate equations are given by

$$e_j + \mathrm{OH}(A)_{i+1} \underset{k'^{i,(+)}_{e,j+1}}{\overset{k^{i+1,(+)}_{e,j}}{\rightleftharpoons}} e_{j+1,(+)} + \mathrm{OH}(A)_i, \qquad (17)$$

$$e_j + \mathrm{OH}(A)_{i} \underset{k'^{i-1,(-)}_{e,j+1}}{\overset{k^{i,(-)}_{e,j}}{\rightleftharpoons}} e_{j+1,(-)} + \mathrm{OH}(A)_{i-1}. \qquad (18)$$

The RET and electronic RET processes produce essentially the same rate equations with different collision partner densities and rate coefficients. Following the same procedure we used previously [27], the time derivative of the diatomic molecule density N_i at rotational state i may be written as

$$\frac{dN_i}{dt} = \left(\frac{dN_i}{dt}\right)^{(+)} + \left(\frac{dN_i}{dt}\right)_e^{(+)} + \left(\frac{dN_i}{dt}\right)^{(-)} + \left(\frac{dN_i}{dt}\right)_e^{(-)}, \qquad (19)$$

where each term in the parentheses corresponds to the net contribution from processes (15), (17), (16), and (18) for the time rate variation of state N_i density. We may proceed by taking the same steps of the derivation in Ref. [27]: (i) Use the microscopic reversibility principle to write the inverse rate coefficients in terms of the direct rate coefficients, (ii) look for the steady-state solution satisfying $dN_i/dt = 0$, and (iii) express the solution in terms of a continuous functions of energy $N(E)$. The final result is the following equation:

$$\frac{dN}{dE} + \frac{N}{k_B T} + \frac{k_e}{k_M}\left(\frac{dN}{dE} + \frac{N}{k_B T_e}\right) = 0, \qquad (20)$$

where T is the temperature of species M, T_e is the electron temperature, k_M is the effective rate of the RET, and k_e the effective rate of the electronic RET. This result shows that if $k_M \gg k_e$ the solution is a Boltzmann equation with temperature T and if $k_e \gg k_M$ the solution is a Boltzmann equation with temperature T_e. This is physically consistent because if the RET dominates over the electronic RET then the rotational temperature should be closer to the gas temperature. If the electronic RET dominates then the opposite is true and the rotational temperature should be closer to the electron gas temperature.

Now let us write the solution for Eq. (20). Before that, it can be readily seen that Eq. (1) is not a solution of Eq. (20). The actual solution is

$$N = N_0 \exp\left[-\int_0^E \frac{dE'}{k_B T(1+\xi)}\right] \times \exp\left[-\int_0^E \frac{dE'}{k_B T_e(1+\xi^{-1})}\right], \qquad (21)$$

where N_0 is the ground state density and $\xi = k_e/k_M$ is what we will call the coupling function. This solution is consistent with the limits we have discussed above. Indeed, if $\xi = k_e/k_M \to \infty$ we recover the Boltzmann distribution with temperature T_e, and if $\xi = k_e/k_M \to 0$ we recover the Boltzmann distribution with temperature T. Note also that Eq. (21) is consistent with Eq. (12) as both are expressed as the product of two-exponential functions, each exponential being a function of one of the temperatures.

In order to use Eq. (21) to model experimental data, we need to know the coupling function $\xi(E)$. It is reasonable to assume, from the previous knowledge we have from this system, that $\xi(E)$ goes to zero in the limit of low energies and goes to infinity in the limit of high energies. We may model $\xi(E)$ as an exponential function, satisfying the previous limits, i.e.,

$$\xi = \xi_0 \exp\left(\frac{E - E_0}{\sigma_0}\right), \qquad (22)$$

---

[1] We will only consider OH(A) molecules in the vibrational ground state, so from now on we will drop ($\nu = 0$) from the notation. We use here the particular case of the OH(A), but this reasoning applies to any electronically excited molecule.

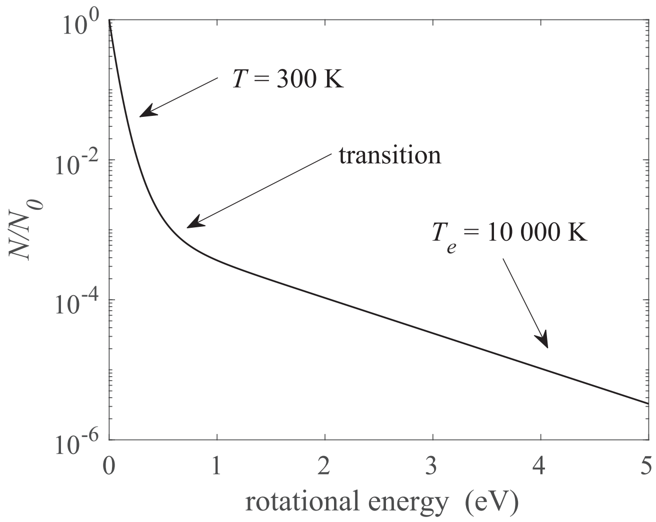

FIG. 2. Plot of the distribution given by Eq. (23), where $T = 300$, $T_e = 10000$ K, $\xi_0 = 100.0$, $E_0 = 1$, and $\sigma_0 = 0.2$ eV.

where ξ_0, E_0, and σ_0 are fitting parameters. Although these are fitting parameters, they give important information about the distribution. For instance, E_0 gives the limit of transition between the two regimes of thermal bath coupling; for $E_0 > E$ the system is better coupled to species M by the RET, and for $E_0 < E$ the system is better coupled to electrons by the electronic RET. The parameter σ_0 gives a measure on how fast this transition occurs. Using the model given above for the coupling function, we may write the density $N(E)$ as

$$N = N_0 \exp\left[-\int_0^E \frac{dE'}{k_B T\left[1 + \xi_0 \exp\left(\frac{E_0 - E}{\sigma_0}\right)\right]}\right] \times \exp\left[-\int_0^E \frac{dE'}{k_B T_e\left(1 + \frac{1}{\xi_0 \exp\left(\frac{E_0 - E}{\sigma_0}\right)}\right)}\right]. \tag{23}$$

The plot of this function is shown in Fig. 2 for the following values of the parameters: $T = 300$, $T_e = 10000$ K, $\xi_0 = 100.0$, $E_0 = 1$, and $\sigma_0 = 0.2$ eV. The shape of the distributions follows the typical trend experimentally observed by many authors [28,29].

III. FITTING PROCEDURE

The model described above was applied to fit some selected experimental spectra, using both the discrete and the continuous approaches. The discrete approach uses Eq. (14) to model the population of the rotational excited states and fit the spectrum, whereas the continuous analysis uses Eq. (23) to fit the Boltzmann plot of a given spectrum. We have chosen UV spectra from plasma emission where the violet OH system was observed. The analysis was restricted to the $0 \rightarrow 0$ band where only the population of rotational states needed to be modeled, and no appreciable contribution of transitions from other bands or systems were observed. In the next section we give more details about the data from which the emission spectra was obtained.

In the discrete case, we used the same method of spectra fitting described in previous works [26,30]. Here we did not need to model the vibrational population as in Ref. [30], but we had to introduce a new function to describe the population of rotational states, based on Eq. (14). The state energies and Holn-London factors were computed using the methods and molecular constants given by Goldman and Gilis [31].

The continuous approach, based on Eq. (23), was used to fit the Boltzmann plot. In order to extract the Boltzmann plot from the spectra, we used the state-to-state fitting method [32–34]. This method basically considers the population of the rotational states as fitting parameters and finds the optimal solution by the least squares method. The rotational occupation number of each rotational state was determined using this method and then used to build the Boltzmann plot.

Besides the two thermal bath model described in this paper, we also fitted the data using the two-exponential sum model [Eq. (1)] for both the spectrum and the Boltzmann plot. The fitting quality and the temperature values were compared with the results from the two thermal bath model.

The fitting routines were implemeted in MATLAB. The codes are available to download in the GitHub repository [35].

IV. EXPERIMENTAL DATA

The $A^2\Sigma^+ \rightarrow X^2\Pi^+$ band spectra of the radical OH were produced by the emission from a negative glow of a DC discharge in a water-cooled hollow cathode (75, 4.0 mm internal diameter), analogous to that used by Callomon [36].

The discharge tube was filled with a flow of a mixture of H_2O (distilled) and N_2 (99.996% purity), at a pressure of 10 torr (1.3 kPa), and operating with a current of approximately 25 mA. A BRUKER IFS 125HR Fourier transform spectrometer ($\approx$2 m optical path difference) at atmospheric pressure, was used to record the UV spectrum of OH. The optical path difference of the equipment is controlled by a stabilized He-Ne laser, which serves as a standard for wave number calibration. The spectrum was recorded at an unapodized resolution of 1.0 cm^{-1}, using a solar blind photomultiplier (Hamamatsu R7154) tube for energies from 30 000 to 50 000 cm^{-1}. No optical filters were placed in front of the detectors.

To ensure the high quality of the measured wave numbers, the spectra have been calibrated using a mercury cadmium spectral lamp (Hg-Cd OSRAM® HgCd/10). The estimated absolute accuracy of our measurements of the transitions is 0.005 cm^{-1} for the strong and unblended lines. The signal to noise ratio (SNR) varied from 8:1 for the weakest lines up to 90:1 for the strongest ones. For weaker lines, the SNR and blending caused by overlapping lines limited the accuracy of measurement to 0.06 cm^{-1}.

V. RESULTS

A. Fitting based on the Boltzmann plot and the continuous distribution

The Boltzmann plot and the fitted curves are shown in Fig. 3. The parameters determined by adjusting the experimental data to the models of two baths and two temperatures are listed in Table I. The full line curve in Fig. 3 is obtained

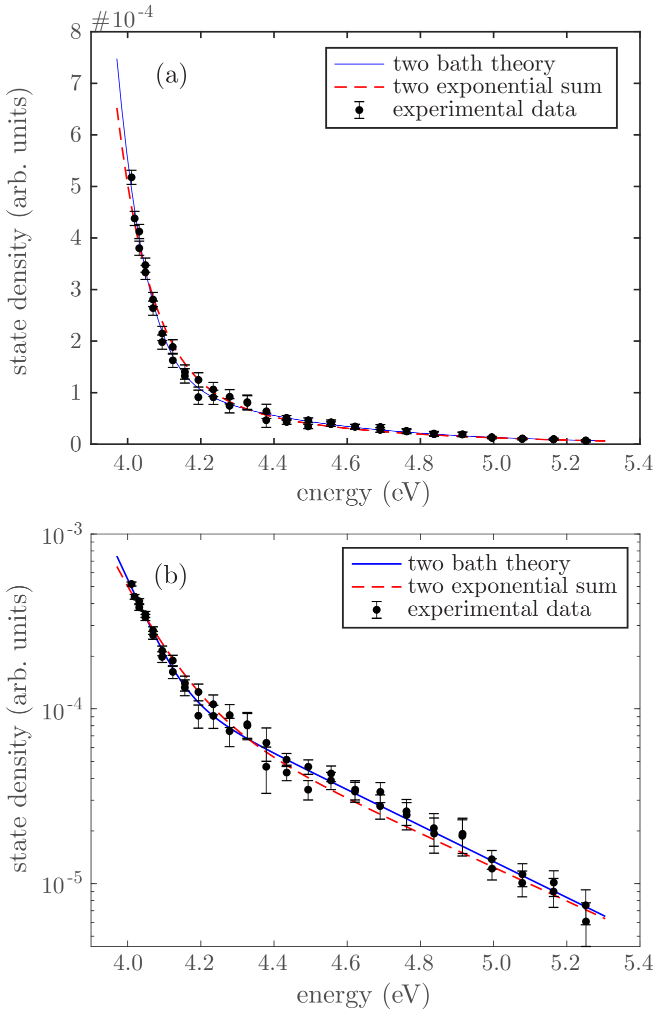

FIG. 3. Boltzmann plot built from a state-to-state algorithm applied to a high resolution spectra of the 0-0 band of the OH violet system. The fitting based on the two bath theory is represented by the full blue line curve whereas the fitting based on the two-exponential sum is represented by the dashed red curve. (a) Plot on the linear scale. (b) Plot on the logarithmic scale.

by fitting the two bath model. The data errors were adjusted by requiring homoscedasticity of the weighted residuals and a resulting χ^2 value within a 5% confidence level. The quality of the fitting is remarkably superior to the fitting based on two-exponential sum fitting. For instance, the residual standard deviation of the former is lower as shown in Table I. Also, the residuals plot in the two bath case show evenly scattered points, whereas the residuals plot in the other case show some trend.

TABLE I. Temperatures T_1, T_2, transition energy E_0, and residual standard deviation σ_{fit} determined from the Boltzmann plot fitting for both models. Fitted values are accompanied by the estimated errors.

	Two bath	Two-exponential sum
T_1 (K)	1116 ± 64	1108 ± 38
T_2 (K)	$(5.90 \pm 0.21) \times 10^3$	$(5.23 \pm 0.17) \times 10^3$
E_0 (eV)	4.334 ± 0.022	
σ_{fit}	1.0×10^{-5}	1.6×10^{-5}

TABLE II. Temperatures T_1, T_2, transition energy E_0, and residual standard deviation σ_{fit} determined from the direct spectra fitting for both models. Fitted values are accompanied by the estimated errors.

	Two bath	Two-exponential sum
T_1 (K)	1239 ± 62	1076 ± 83
T_2 (K)	$(4.5 \pm 0.3) \times 10^3$	$(8.75 \pm 1.0) \times 10^3$
E_0 (eV)	4.247 ± 0.025	
σ_{fit}	4.49×10^{-2}	4.51×10^{-2}

The two-exponential sum model may be rejected considering the present data. Despite that, the estimated values for T_1 and T_2 in the two-exponential sum is statistically compatible with the corresponding parameters estimated using the two bath theory. It suggests that the two-exponential model may not give the best fit, but it could eventually yield consistent estimates for the temperatures.

We will now discuss if the estimated values for the temperatures are reasonable. By comparing these values with reported results from literature, we see that the estimated value for the T_1 temperature $T_1 = 1116 \pm 64$ K is consistent with typical gas temperatures in the bulk of low pressure hollow cathode discharge at similar operating pressures [37]. The higher temperature $T_2 = (0.508 \pm 0.018)$ eV, converted here to eV, is also consistent with typical electron temperatures found in similar discharges [37]. Therefore, we may associate the T_1 temperature with the gas temperature and the T_2 temperature with the electron temperature. We should not discard other interactions contributing to the shaping of the highly populated tail of the distribution, and the T_2 may be an effective temperature resulting from interactions with other species besides the electrons. What we may say for now is that the distribution seems to behave as if governed by two independent thermal baths with different temperatures.

B. Fitting based on the rovibrational spectrum and the discrete distribution

The emission spectra dominated by the $\nu' = 0 \rightarrow \nu = 0$ OH violet band is shown in Fig. 4 where both fitting curves are presented in separate plots. In this case we did not note appreciable differences between the models, although the fitting based on the two bath theory yielded a lower standard deviation of residuals. We note in both plots that *R*-branch lines are consistently underestimated. The same was observed in the state-to-state fitting. This result suggests that there may be some inaccuracy in the Honl-London factors, which may be due to the limitations of commonly used approximations, such as the Born-Oppenheimer approximation. However, the *Q* and *P* branches are described reasonably well by both fittings.

Table II shows the temperatures and other parameters from both fittings. The values of the discrete fitting are compatible with the values of the continuous fitting, showing consistency between both approaches. The T_2 temperature determined using the two-exponential sum is numerically higher than its

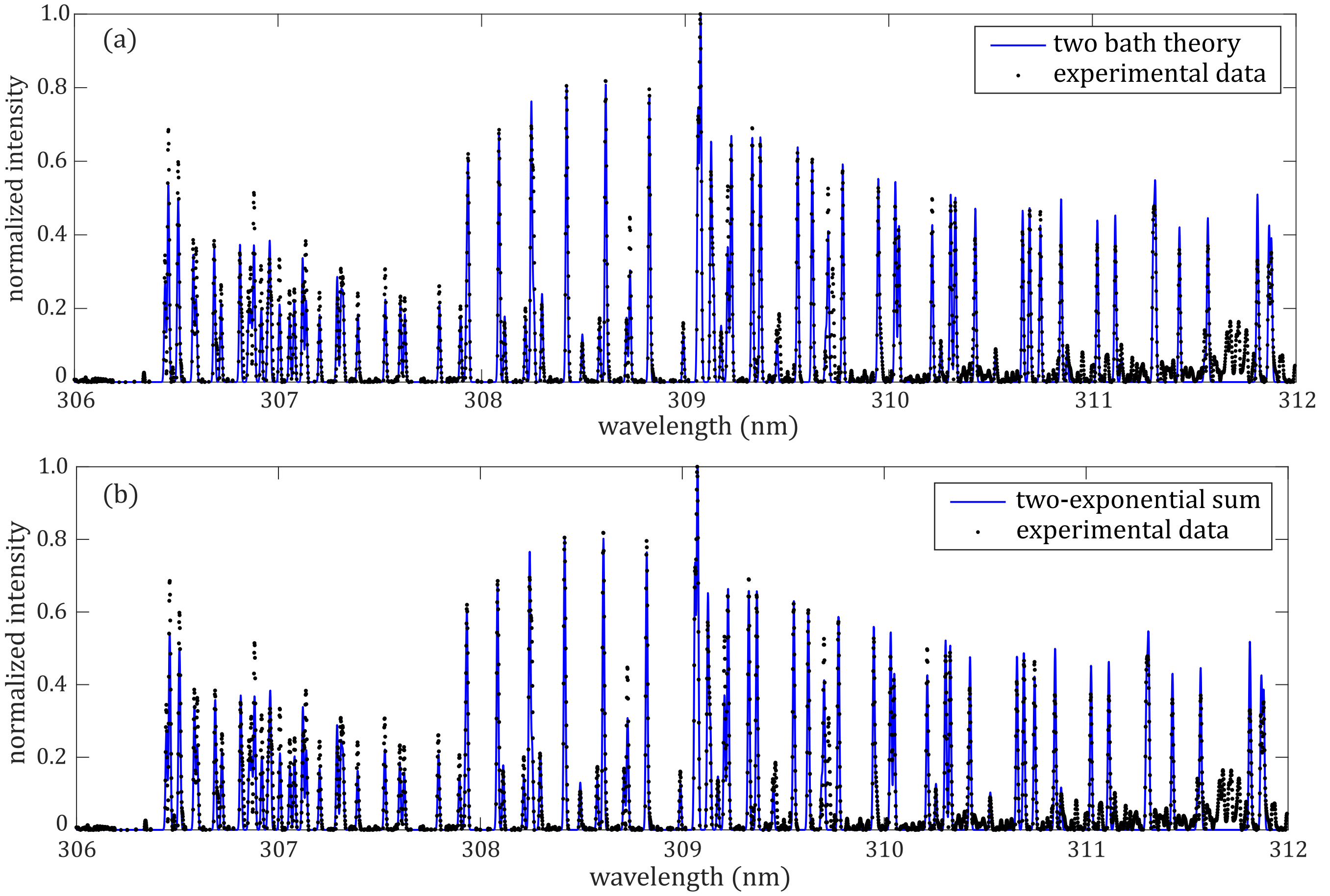

FIG. 4. Spectra fitting of a high resolution spectra 0-0 band of the OH violet system. Plot (a) fitting based on the two bath theory. Plot (b) fitting based on the two-exponential sum model.

counterpart in the continuous fitting (Table I), but the uncertainty is large enough to explain the difference.

C. Discussion

We may ask now, in light of the present theory, which method should be used in ordinary and routine experimental evaluations of plasma temperature by means of OH violet spectra. If the goal is only the determination of the gas temperature, the theory ensures that T_1 values should have the best correspondence to the gas translational temperature. The theory shows that states with very low J values may be almost uninfluenced by the second thermal bath as long as the σ_0 parameter is not too large. This means that, in principle, one could select only low J states resulting in straight lines in the Boltzmann plot or very good fittings of the spectra. In these cases, it is possible to simply assume that state occupancy is governed by the Boltzmann distribution, provided that this assumption is restricted to states with low J values. If the spectra is too entangled due to low resolution and the peaks cannot be easily estimated, the state-to-state fitting is recommended if one wishes to make use of the Boltzmann plot to estimate the temperature. Besides, depending on the shape of the distribution, there may not be a well defined straight line in the low energy sector of the Boltzmann plot. In terms of the present theory, this could happen for large values of the parameter σ_0 or $\tilde{\sigma}_0$. In this case, a fitting using the two bath theory would be preferred rather than arbitrarily selecting a threshold J value.

One could eventually ask if the current theory could be used to estimate the electron temperature. Although the theory predicts this possibility, it would only be valid if the high energy sector of the OH rotational distribution was governed only by interactions with electrons. This means that this method cannot be used to estimate directly the electron temperature, although it can be used in routine measurements if the correlation or equivalence with electron temperature is previously assessed using an accurate measurement technique.

Although the application of the theory was restricted to the analysis of the OH violet spectra, it can be applied to any rovibrational spectra generated by plasmas where similar behavior may occur. The OH spectra have the advantage of being common in plasmas and having well separated lines. The application of the present theory on other molecular spectra will be explored in future works.

VI. CONCLUSION

In this paper we derived the distribution of rotational states of diatomic molecules in a medium where they can be modeled as a subsystem interacting with two distinct and uncoupled thermal baths. This theory is particularly suitable to describe the rotational distribution of diatomic molecules in low temperature and weakly ionized plasmas where each thermal bath may be interpreted as a population of species in the plasma that interacts with the molecules—e.g., neutral atoms and molecules in the ground state, electrons, etc. A discrete version of the rotational distribution function was derived using the principle of maximum entropy and constraints consistent with the problem. We also derived a continous version of the rotational distribution function using the master equations and detailed balancing. We showed that the two distribution functions are equivalent.

We applied the present method in the analysis of a high resolution rovibrational spectra of the OH violet system, produced by the emission of a low-pressure DC hollow cathode discharge. Using the state-to-state method we obtained the Boltzmann plot, and we demonstrated that the present theory gives a better description of the experimental data than the conventional procedure of describing the distribution as a sum of two Boltzmann distributions with different temperatures. In light of the present theory, we showed that the lower temperature, associated with the colder bath, should be interpreted as an estimate of the translational energy of the gas. The higher temperature, on the other hand, should be interpreted as an estimate of the effective temperature of the more energetic species, such as electrons and excited species. Therefore, the method we propose here is specially relevant for the study and diagnostics of low temperature and weakly ionized plasmas where heavy species and electrons kinetic energies are not equipartitioned and electron mean energies are much higher.

ACKNOWLEDGMENTS

This research has been supported by Project No. LM2018097 by the Ministry of Education, Youth and Sports of the Czech Republic. It has also been supported by Project No. 16/24970-7 by FAPESP (Fundação de Amparo à Pesquisa do Estado de São Paulo).

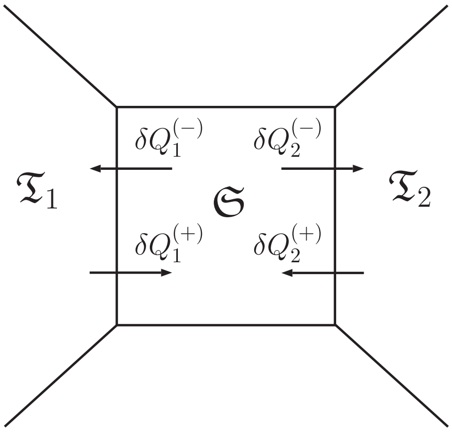

FIG. 5. Representation of the energy exchange between system $\mathfrak{S}$ and baths $\mathfrak{T}_1$ and $\mathfrak{T}_2$. We assume that for a given small time interval, heat amounts $\delta Q_1^{(+)}$ and $\delta Q_2^{(+)}$ are introduced into the system by thermal baths $\mathfrak{T}_1$ and $\mathfrak{T}_2$, and heat amounts $\delta Q_1^{(-)}$ and $\delta Q_2^{(-)}$ are removed from the system by thermal baths $\mathfrak{T}_1$ and $\mathfrak{T}_2$.

APPENDIX A: PARTIAL INTERNAL ENERGIES ARE WELL DEFINED AND MEASURABLE QUANTITIES

Let us assume that the internal energy $U(t)$ of the system $\mathfrak{S}$ coupled to two thermal baths is given, at any instant, by the sum of the energy introduced by thermal bath $\mathfrak{T}_1$ and the energy introduced by thermal bath $\mathfrak{T}_2$ so that $U(t) = U_1(t) + U_2(t)$. Energy U_i is defined as the internal energy content which was introduced in the system by thermal bath $\mathfrak{T}_i$ exclusively. For any instant of time, the value of U_i may be increased by the energy input from $\mathfrak{T}_i$ or may be decreased by energy loss for both thermal baths. Therefore, the energy budget equation may be written as

$$\frac{dU_1}{dt} = \frac{dQ_1^{(+)}}{dt} - \frac{dQ_{11}^{(-)}}{dt} - \frac{dQ_{12}^{(-)}}{dt}, \tag{A1a}$$

$$\frac{dU_2}{dt} = \frac{dQ_2^{(+)}}{dt} - \frac{dQ_{21}^{(-)}}{dt} - \frac{dQ_{22}^{(-)}}{dt}, \tag{A1b}$$

where $dQ_1^{(+)}/dt$ and $dQ_2^{(+)}/dt$ are the input heat flows from thermal baths $\mathfrak{T}_1$ and $\mathfrak{T}_2$, $dQ_{11}^{(-)}/dt$, and $dQ_{12}^{(-)}/dt$ are the output heat flows to thermal baths $\mathfrak{T}_1$ and $\mathfrak{T}_2$, respectively, decreasing U_1 internal energy, and $dQ_{21}^{(-)}/dt$ and $dQ_{22}^{(-)}/dt$ are the output heat flows to thermal baths $\mathfrak{T}_1$ and $\mathfrak{T}_2$, decreasing U_2 internal energy. Figure 5 gives a schematic of the system energy exchange. In this equation, we assumed that the net input heat from the thermal baths is entirely converted into internal energy. Before the stationary equilibrium is reached, the net heat flow could also be negative, depending on the instantaneous state of the system. Since the thermal baths are assumed ideal, the energy input is constant and depends only on the temperature and entropy loss rate of the thermal bath, i.e.,

$$\frac{dQ_1^{(+)}}{dt} = \Gamma_1^{(+)}(T_1) = \text{cte.}, \tag{A2a}$$

$$\frac{dQ_2^{(+)}}{dt} = \Gamma_2^{(+)}(T_2) = \text{cte.}, \tag{A2b}$$

where $\Gamma_i^{(+)}(T_i)$ is the constant energy input from thermal bath $\mathfrak{T}_i$, which depends only on the temperature and the coupling characteristics of the thermal bath, but not on time or the state of system $\mathfrak{S}$. Analogously, we may write the energy loss of the system to the thermal baths as

$$\frac{dQ_1^{(-)}}{dt} = \frac{dQ_{11}^{(-)}}{dt} + \frac{dQ_{21}^{(-)}}{dt} = \Gamma_1^{(-)}(t), \tag{A3a}$$

$$\frac{dQ_2^{(-)}}{dt} = \frac{dQ_{12}^{(-)}}{dt} + \frac{dQ_{22}^{(-)}}{dt} = \Gamma_2^{(-)}(t), \tag{A3b}$$

where $\Gamma_1^{(-)}(t)$ and $\Gamma_2^{(-)}(t)$ are now functions that may depend on time and state of system $\mathfrak{S}$. We now assume that in the limit of long times after some initial condition, the system will reach stationary equilibrium, which requires that

$$\lim_{t\to\infty} \Gamma_1^{(-)}(t) = -\Gamma_1^{(+)}, \tag{A4a}$$

$$\lim_{t\to\infty} \Gamma_2^{(-)}(t) = -\Gamma_2^{(+)}. \tag{A4b}$$

We will also assume that heat flows are slow and the system evolves towards stationary equilibrium slowly so that internal energy $U(t)$ varies uniformly.[2] After some introduction of heat from the thermal baths we may consider that heat energies are equally partitioned among every subsystem. Therefore, any subsystem should have the same proportion of U_1 and U_2 at a given time t, although this proportion may uniformly change in time. The prior assumptions allow us to write the energy losses as

$$\frac{dQ_{11}^{(-)}}{dt} + \frac{dQ_{12}^{(-)}}{dt} = \nu_1 U_1 + \nu_2 U_1, \tag{A5a}$$

$$\frac{dQ_{21}^{(-)}}{dt} + \frac{dQ_{22}^{(-)}}{dt} = \nu_1 U_2 + \nu_2 U_2, \tag{A5b}$$

where we introduced the rate coefficient ν_i which quantifies how fast heat is transferred from system $\mathfrak{S}$ to thermal bath $\mathfrak{T}_i$. This quantity depends on the properties of the thermal bath and its coupling to system $\mathfrak{S}$ and should be strictly positive, greater than zero and should not depend explicitly on time. We may now rewrite Equations (A1a) and (A1b) as a system of first order ordinary differential equations,

$$\frac{dU_1}{dt} = \Gamma_1^{(+)} - (\nu_1 + \nu_2)U_1, \tag{A6a}$$

$$\frac{dU_2}{dt} = \Gamma_2^{(+)} - (\nu_1 + \nu_2)U_2. \tag{A6b}$$

These equations are uncoupled and can be solved separately using well known analytical methods. We will impose the initial condition at some time t_0—arbitrarily set to zero ($t_0 = 0$)—for which the initial internal energy is known and given by $U_1(t_0) = U_{10},\ U_2(t_0) = U_{20}$, and $U(t_0) = U_{10} + U_{20}$. The solution for this differential equation for this initial condition is given by

$$U_i(t) = \frac{U_{i0}}{\mu(t)} + \frac{\Gamma_i^{(+)}}{\mu(t)} \int_0^t \mu(t')dt', \tag{A7}$$

where i is the index of the thermal bath (e.g., 1 for thermal bath $\mathfrak{T}_1$) and $\mu(t) = \exp[(\nu_1 + \nu_2)t]$. Let us now take the limit $t \to \infty$ of the equation above. Before that, we should note that $\mu(t) \to \infty$ as $t \to \infty$, so the first term of the right hand side of Eq. (A7) will be zero. So all we need to do now is to compute the limit of the second term. It can be readily seen that both the integral in the numerator and the function in the denominator go to infinity, so we may apply the l'Hôpital rule to compute it,

$$\lim_{t\to\infty} U_i(t) = \lim_{t\to\infty} \frac{\zeta'(t)}{\mu'(t)} = \lim_{t\to\infty} \frac{\Gamma_i^{(+)}\mu(t)}{(\nu_1 + \nu_2)\mu(t)} = \frac{\Gamma_i^{(+)}}{(\nu_1 + \nu_2)}, \tag{A8}$$

where $\zeta(t) = \Gamma_i^{(+)} \int_0^t \mu(t')dt'$ and use was made of the Leibnitz rule to compute the derivative of the integral function $\zeta(t)$. We immediately conclude from the above limit that the partial internal energy U_i converges to a constant value which does not depend on the initial condition nor the thermodynamic path. This constant value depends on the heat input flow from the bath and the heat flow rate coefficients from both baths. The condition of stationary equilibrium allow us to write ν_i as a function of the total internal energy and the input heat flow of the ith thermal bath, i.e., $\nu_i = \Gamma_i^{(+)}/U_{\text{eq}}$. Substitution on Eq. (A8) gives us the equilibrium energy $U_{i,\text{eq}}$,

$$U_{i,\text{eq}} = U_{\text{eq}} \frac{\Gamma_i^{(+)}}{\sum_j \Gamma_j^{(+)}}. \tag{A9}$$

The sum in the denominator of this equation is just the sum of the heat flow input from the two thermal baths, but we see that this result may be readily generalized to any number of thermal baths. The ratio between the partial value $U_{i,\text{eq}}$ and the total internal energy is nothing but the ratio between the input heat flow of the ith thermal bath and the total input heat flow. Since the heat flow from an ideal thermal bath may be assumed constant, one may clearly see that the value of $U_{i,\text{eq}}$ is unique in thermal equilibrium conditions. In our derivation of the rotational energy distribution function in Sec. II, this thermal equilibrium state was implicitly assumed. This means that the energies U_1 and U_2 should be interpreted as the equilibrium energies $U_{1,\text{eq}}$ and $U_{2,\text{eq}}$. Since these quantities have well defined mean values, which depend only on the thermal bath characteristics, they can be used as constrained quantities in the entropy maximization procedure. We also note that the partial derivatives of the entropy S from Eqs. (2a) and (2b) must be interpreted as a derivative in the domain of equilibrium values $U_{1,\text{eq}}$ and $U_{2,\text{eq}}$. This is valid since we search a solution after the stationary equilibrium is reached. Again, we recall that stationary equilibrium is defined here as the condition where the net exchange of heat is zero, and system $\mathfrak{S}$ may not have a well defined temperature.

APPENDIX B: RELATION OF THE PRESENT THEORY TO SUPERSTATISTICS

We include here a brief note on the relation of the present theory with superstatistics. Superstatistics describe systems where temperature may fluctuate and whose value is not unique, although some value may be eventually measured within some prescribed distribution [38]. One may ask if the present theory could eventually be easily related to the formalism of superstatistics. Although a detailed analysis of this question is outside the scope of the present paper we think that some discussion about this would be worthwhile for a greater audience. Superstatistics describes systems where temperature may fluctuate in timescales greater than the relaxation time. The temperature value can be measured but may vary according to some prescribed distribution. This would be the case, for instance, in an experiment that measures temperature from light emitted from two distinct and uncoupled plasmas in the same line of sight of the apparatus. It could also be a time resolved measurement of an oscillating plasma alternating between two equilibrium states. In these

---

[2] The system as a whole (system $\mathfrak{S}$ plus thermal baths) may not be in thermal equilibrium, but the internal energy is supposed to have a uniform and well defined mean value for every instant t. The stationary equilibrium is reached when the net heat exchange in any given thermal bath is zero, a condition usually referred to as zeroth thermodynamic law. This condition is also assumed in the conventional case of thermal equilibrium for one thermal bath, but in the case of two or more thermal baths, system $\mathfrak{S}$ may not have a well defined temperature.

cases, the temperature probability distribution function could be simply two Dirac δ's, one centered at T_1 and the other centered at T_2. Analogously, we may consider another experiment where the emission of a plasma is also measured, but for some reason some microscopic states of the plasma couple only to one thermal bath and the other couple only to the other thermal bath. In this case, our distribution could be defined as a conditional Dirac δ, depending on some energy threshold. However, in general, our problem is different. It is not only that the temperature may fluctuate in time or space; actually, the system temperature is not well defined, and it cannot be measured except for some special cases. Only the thermal bath temperatures are well defined, and we may only allow fluctuations of these temperatures. For this reason, maybe the usual "univariate" expression for Z in conventional superstatistics may have to be generalized to a "multivariate" expression to describe systems similar to ours, e.g., $Z = \iint f(\beta_1, \beta_2) \exp(-\beta_1 E) \exp(-\beta_2 E) d\beta_1 d\beta_2$. This should not be seen as a definitive answer, but it may guide new developments if the present theory indeed could find more applications beyond the specific problem of diatomic rotational distributions in plasmas.

[1] G. Dieke and H. Crosswhite, J. Quant. Spectrosc. Radiat. Transfer **2**, 97 (1962).

[2] H. W. Drawin, in *Reactions Under Plasma Conditions*, edited by M. Venugopalan (Wiley-Interscience, New York/London/Sydney/Toronto, 1971).

[3] A. Fridman, *Plasma Chemistry* (Cambridge University Press, Cambridge, UK, 2008).

[4] M. A. Ridenti, J. de Amorim, and A. Dal Pino, IEEE Trans. Plasma Sci. **43**, 4066 (2015).

[5] M. A. Lieberman and A. J. Lichtenberg, *Principles of Plasma Discharges and Materials Processing* (Wiley, Hoboken, NJ, 2005).

[6] Y. P. Raizer, *Gas Discharge Physics*, 1st ed. (Springer, 1997).

[7] E. Gerjouy and S. Stein, Phys. Rev. **97**, 1671 (1954).

[8] N. F. Mott and H. S. W. Massey, *The Theory of Atomic Collisions*, 2nd ed. (Oxford University Press, London, 1950).

[9] M. D. Calzada, M. Moisan, A. Gamero, and A. Sola, J. Appl. Phys. **80**, 46 (1996).

[10] K. Kumar, H. Skullerud, and R. E. Robson, Aust. J. Phys. **33**, 343 (1980).

[11] L. M. Biberman, V. S. Vorob'ev, and I. T. Yakubov, *Kinetics of Nonequilibrium Low-Temperature Plasmas*, 1st ed. (Springer, New York, 1987).

[12] E. Carbone, S. Hübner, M. Jimenez-Diaz, J. Palomares, E. Iordanova, W. Graef, A. Gamero, and J. van der Mullen, J. Phys. D: Appl. Phys. **45**, 475202 (2012).

[13] M. A. Ridenti, V. Guerra, and J. Amorim, in *Plasma Modeling*, edited by G. Colonna and A. D'Angola (IOP, Bristol, 2016), 2053–2563, Chap. 11.

[14] J. Amorim, M. A. Ridenti, and V. Guerra, Plasma Phys. Controlled Fusion **57**, 074001 (2015).

[15] M. A. Ridenti, J. de Amorim, A. Dal Pino, V. Guerra, and G. Petrov, Phys. Rev. E **97**, 013201 (2018).

[16] G. J. M. Hagelaar and L. C. Pitchford, Plasma Sources Sci. Technol. **14**, 722 (2005).

[17] S. D. Rockwood, Phys. Rev. A **8**, 2348 (1973).

[18] A. Lofthus and P. H. Krupenie, J. Phys. Chem. Ref. Data **6**, 113 (1977).

[19] V. Linss, Spectrochim. Acta, Part B **60**, 253 (2005).

[20] V. Linss, H. Kupfer, S. Peter, and F. Richter, J. Phys. D: Appl. Phys. **37**, 1935 (2004).

[21] E. Jaynes, *Frontiers of Nonequilibrium Statistical Physics* (Springer, Berlin, 1986), pp. 33–55.

[22] R. Luzzi, Á. R. Vasconcellos, and J. G. Ramos, *Predictive Statistical Mechanics: A Nonequilibrium Ensemble Formalism* (Springer, Berlin, 2013), Vol. 122.

[23] R. Balian, *Theoretical an Mathematical Physics. From Microphysics to Macrophysics* (Springer, Berlin, 2007), Vol. 1.

[24] J. C. Polanyi and K. B. Woodall, J. Chem. Phys. **56**, 1563 (1972).

[25] P. Bruggeman and D. C. Schram, Plasma Sources Sci. Technol. **19**, 045025 (2010).

[26] J. L. Reis, J. Amorim, and A. Dal Pino, Phys. Rev. E **83**, 017401 (2011).

[27] M. A. Ridenti, J. de Amorim, and A. Dal Pino, Phys. Rev. E **99**, 033202 (2019).

[28] P. Bruggeman, N. Sadeghi, D. Schram, and V. Linss, Plasma Sources Sci. Technol. **23**, 023001 (2014).

[29] M. A. Ridenti, J. A. Souza-Corrêa, and J. Amorim, J. Phys. D: Appl. Phys. **47**, 045204 (2014).

[30] M. Ridenti and J. Amorim, Plasma Chem. Plasma Process. **38**, 311 (2018).

[31] A. Goldman and J. R. Gillis, J. Quant. Spectrosc. Radiat. Transfer **25**, 111 (1981).

[32] J. Voráč, P. Synek, V. Procházka, and T. Hoder, J. Phys. D: Appl. Phys. **50**, 294002 (2017).

[33] J. Voráč, P. Synek, L. Potočňáková, J. Hnilica, and V. Kudrle, Plasma Sources Sci. Technol. **26**, 025010 (2017).

[34] J. Voráč, L. Kusýn, and P. Synek, Rev. Sci. Instrum. **90**, 123102 (2019).

[35] The GitHub repository, https://github.com/mridenti/two_bath_fitting.

[36] J. H. Callomon, Proc. R. Soc. London, Ser. A: Math. Phys. Sci. **244**, 220 (1958).

[37] E. Van Veldhuizen and F. De Hoog, J. Phys. D: Appl. Phys. **17**, 953 (1984).

[38] C. Beck and E. G. Cohen, Physica A **322**, 267 (2003).

Correction: The label for the blue line in the legend of Figure 4(b) was incorrect and has been fixed.